Microbiology (2013), **159**, 205–218 DOI 10.1099/mic.0.061937-0

A constitutively expressed pair of *rpoE2–chrR2* in *Azospirillum brasilense* Sp7 is required for survival under antibiotic and oxidative stress

Namrata Gupta, Santosh Kumar, Mukti Nath Mishra and Anil Kumar Tripathi

School of Biotechnology, Faculty of Science, Banaras Hindu University, Varanasi-221005, India

Correspondence
Anil Kumar Tripathi
tripathianil@rediffmail.com

Received 5 July 2012
Revised 21 September 2012
Accepted 4 October 2012

Extracytoplasmic function (ECF) sigma factors (σ^E) are known to bring about changes in gene expression to enable bacteria to adapt to different stresses. The *Azospirillum brasilense* Sp245 genome harbours nine genes encoding σ^E, of which two are adjacent to the genes encoding ChrR-type zinc-binding anti-sigma (ZAS) factors. We describe here the role and regulation of a new pair of *rpoE–chrR*, which was found in the genome of *A. brasilense* Sp7 in addition to the previously described *rpoE–chrR* pair (designated *rpoE1–chrR1*). The *rpoE2–chrR2* pair is also cotranscribed, and their products show protein–protein interaction. The −10 and −35 promoter elements of *rpoE2–chrR2* and *rpoE1–chrR1* were similar but not identical. Unlike the promoter of *rpoE1–chrR1*, the *rpoE2–chrR2* promoter was neither autoregulated nor induced by oxidative stress. Inactivation of *chrR2* or overexpression of *rpoE2* in *A. brasilense* Sp7 resulted in an overproduction of carotenoids. It also conferred resistance to oxidative stresses and antibiotics. By controlling the synthesis of carotenoids, initiation and elongation of translation, protein folding and purine biosynthesis, RpoE2 seems to play a crucial role in preventing and repairing the cellular damage caused by oxidative stress. Lack of autoregulation and constitutive expression of *rpoE2–chrR2* suggest that RpoE2–ChrR2 may provide a rapid mechanism to cope with oxidative stress, wherein singlet oxygen ($^1O_2$)-mediated dissociation of the RpoE2–ChrR2 complex might release RpoE2 to drive the expression of its target genes.

INTRODUCTION

Azospirillum brasilense, a Gram-negative, plant-growth-promoting α-proteobacterium of the family *Rhodospirillaceae*, lives in association with the rhizosphere of a large number of non-leguminous plants and brings about plant growth promotion via the production of phytohormones and siderophores (Baldani *et al.*, 1979; Steenhoudt & Vanderleyden, 2000). Bacteria inhabiting the soil and rhizosphere frequently encounter fluctuations in osmolarity, temperature, pH, nutrients, reactive oxygen species and other abiotic factors. They have evolved mechanisms to respond and adapt to such environmental contingencies (Park *et al.*, 2008; Steenhoudt & Vanderleyden, 2000). This is achieved by the reversible association of different σ factors with bacterial RNA polymerase to alter the pattern of gene expression by changing the affinity and specificity of RNA polymerase for different promoters (Helmann, 2002).

Abbreviations: ASD, anti-sigma domain; CLD, cupin-like domain; ECF, extracytoplasmic function; Ni-NTA, nickel-nitrilotriacetic acid; $^1O_2$, singlet oxygen; RACE, random amplification of cDNA ends; TSS, transcription start site; ZAS, zinc-binding anti-sigma.

Five supplementary figures and a supplementary table are available with the online version of this paper.

The extracytoplasmic function (ECF) sigma factors (σ^E) belong to the largest and the most diverse subfamily of σ factors, which is involved in a wide range of stress adaptations (Alvarez-Martinez *et al.*, 2007; Anthony *et al.*, 2005; Bang *et al.*, 2005; Firoved *et al.*, 2002; Martínez-Salazar *et al.*, 2009; Rowley *et al.*, 2006; Schurr *et al.*, 1996). The activity of an ECF sigma factor is often regulated by its association with an anti-sigma factor that receives diverse signals via different mechanisms (Helmann, 2002). After receiving a stimulus, the anti-sigma factor is released from the sigma factor, which can bind together with the core enzyme to the promoter regions of specific genes to drive their transcription. Most often, ECF sigma factor-encoding genes are organized in an operon along with an anti-sigma factor-encoding gene located downstream (Brown & Hughes, 1995; Mishra *et al.*, 2011; Staroń *et al.*, 2009). Most of the anti-sigma factors possess a well-conserved N-terminal anti-sigma domain (ASD), which is involved in the sequestering of the ECF sigma factor to prevent it from binding to the RNA polymerase core enzyme. The anti-sigma factors, such as RseA of *Escherichia coli*, are integral cytoplasmic membrane proteins with a C-terminal extracytoplasmic sensory domain and an N-terminal intracellular inhibitory domain that binds and inhibits the cognate

σ factor (Helmann, 2002; Rowen & Deretic, 2000; Yoshimura *et al.*, 2004). The cytosolic anti-sigma factors, such as RsrA of *Streptomyces coelicolor* (Paget *et al.*, 2001) and ChrR of *Rhodobacter sphaeroides* (Anthony *et al.*, 2004; Newman *et al.*, 2001), belong to the zinc-binding anti-sigma (ZAS) family of anti-sigma factors, and possess a conserved $HisX_3CysX_2Cys$ Zn^{2+}-binding motif in the N-terminal ASD.

The role of the alternative sigma factor σ^E and its cognate anti-sigma factor ChrR in mounting a transcriptional response to photooxidative stress has been characterized in detail in *Rhodobacter sphaeroides* (Glaeser *et al.*, 2011; Ziegelhoffer & Donohue, 2009). In the absence of singlet oxygen ($^1O_2$), ChrR forms a 1:1 complex with σ^E, preventing the σ factor from binding to the core RNA polymerase and initiating transcription of the target genes. In the presence of $^1O_2$, σ^E is released from ChrR and triggers the expression of genes needed for protection against photooxidative stress (Glaeser *et al.*, 2011; Greenwell *et al.*, 2011). The genes controlled by σ^E and their target promoters in *R. sphaeroides* revealed that the members of the σ^E regulon and their promoter consensus in several α-proteobacteria might be common (Dufour *et al.*, 2008; Ziegelhoffer & Donohue, 2009). In spite of the fact that carotenoids are efficient scavengers of $^1O_2$ (Glaeser & Klug, 2005), their synthesis in *R. sphaeroides* is not controlled by σ^E (Anthony *et al.*, 2005).

We have earlier described a σ^E/anti-sigma pair in *A. brasilense* in which the anti-sigma factor showed homology to a ZAS-family anti-sigma factor, ChrR, of *R. sphaeroides* (Mishra *et al.*, 2011). This σ^E–anti-sigma pair controls carotenoid biosynthesis as well as tolerance to elevated temperature, salinity, ethanol, PEG-200, polymixin B and methylene blue in *A. brasilense* (Mishra *et al.*, 2008, 2011; Thirunavukkarasu *et al.*, 2008). We found another ZAS-family anti-sigma factor (AZOBR_p1140122) encoded downstream of a gene encoding an ECF sigma factor (AZOBR_p1140121) in the 7.5 Mb large genome of *A. brasilense* Sp245 (Wisniewski-Dyé *et al.*, 2011). Since the occurrence and role of more than one ZAS-family anti-sigma factor have not, to our knowledge, been reported in any Gram-negative bacterium so far, this study was undertaken to examine the role and regulation of the second pair of RpoE and ChrR in *A. brasilense*.

METHODS

Bacterial strains, plasmids and culture media. Bacterial strains and plasmids used in this study are shown in Table 1. *A. brasilense* Sp7 and its derivative strains were grown in Luria–Bertani (LB) medium or minimal medium (MMAB) containing malate (40 mM) and NH_4Cl (10 mM) as the sole source of carbon and nitrogen, respectively (Vanstockem *et al.*, 1987), at 30 °C with shaking at 150 r.p.m. *E. coli* strains, including *E. coli* DH5α, were grown at 37 °C in LB medium supplemented with 100 μg ampicillin ml^{-1} (Amp), 40 μg kanamycin ml^{-1} (Km), 25 μg chloramphenicol ml^{-1} (Cm) and 15 μg tetracyline ml^{-1} (Tc). The growth of *A. brasilense* strains was monitored by measuring OD_{600}. All the chemicals used for growing bacteria and antibiotics used for the disk diffusion assay were from HiMedia. Restriction enzymes used for DNA manipulations and cloning were from New England Biolabs.

Bioinformatic analysis. BLAST (http://blast.ncbi.nlm.nih.gov/Blast.cgi) was used for homology searches, CLUSTAL W (http://www.ebi.ac.uk/Tools/msa/clustalw2/) for generating multiple sequence alignments, MEGA 5.04 for constructing Neighbour Joining (NJ) phylogenetic trees, OligoAnalyzer 3.1 (http://www.idtdna.com/analyzer/Applications/OligoAnalyzer/) for primer design, and Vector NTI Advance 10 (Invitrogen) for the construction of genetic maps of different loci and to analyse nucleotide and amino acid sequences. Primers used in this study are listed in Table S1 available with the online version of this paper. The BioProspector (Liu *et al.*, 2001) algorithm was used to search for a putative promoter motif within 500 bp upstream regions of translational start sites of protein-coding genes identified in the 2D gel. The parameters were set to search for two blocks of 6 bp and for a gap of 17–19 bp. The resulting sequence motifs were illustrated based on multiple sequence alignment using the WebLogo3 tool at http://weblogo.berkeley.edu (Crooks *et al.*, 2004).

RNA extraction and RT-PCR analysis. Total RNA extraction from *A. brasilense* Sp7 and RT-PCR were performed as described previously (Mishra *et al.*, 2011).

Determination of transcription start sites (TSSs). The 5′ end of the mRNA was mapped from a 5′ random amplification of cDNA ends (RACE) using the 3′/5′ RACE kit, 2nd Generation (Roche) according to the manufacturer's protocol. The *rpoE2* transcript was reverse-transcribed into cDNA using an *rpoE2* gene-specific primer, GSP1 (*rpoE2*-R, Table S1). The cDNAs were purified and poly(dA)-tailed at their 3′ ends. Poly(dA)-tailed cDNA was PCR-amplified using the oligo dT-anchor primer provided by the kit to anneal at the poly(dA) tail and the GSP2 primer (Table S1), complementary to a region upstream of the GSP1-binding site. The PCR product was used as the template in a second PCR using the anchor primer to anneal at a region generated by the oligo dT-anchor primer at the 3′ end of the cDNA and a distinct gene-specific *rpoE2* nested primer GSP3 (Table S1), which was further complementary to a region upstream of the GSP2-binding site. The amplified products obtained from the second PCR were ligated into the pGEM-T Easy vector (Promega), and the nucleotide sequences of several distinct clones were determined in an ABI-PRISM 310 Genetic Analyzer (Applied Biosystems) using T7 forward and Sp6 reverse universal primers.

Pull-down assay. The full-length *rpoE2–chrR2* gene pair of *A. brasilense* Sp7 was PCR-amplified using the *rpoE2*-F1/*chrR2*-R1 primer pair (Table S1) and cloned into the *Nde*I–*Bam*HI site of pET15b. The resulting plasmid (pNG2) was transformed in *E. coli* BL21λ (DE3) pLysS. The nucleotide sequence of the insert of pNG2 was determined as described above. All the conditions used for coexpression and the pull-down assay have been described previously (Mishra *et al.*, 2011). Proteins eluted after nickel-nitrilotriacetic acid (Ni-NTA) affinity purification were trypsin-digested and identified by MALDI-TOF/TOF.

Two-hybrid assay. The two-hybrid assay to study *in vivo* the protein–protein interaction between RpoE2 and ChrR2 was carried out as described previously (Mishra *et al.*, 2011) using the BacterioMatch II Two-Hybrid system (Agilent). Briefly, the *rpoE2* and *chrR2* genes were amplified using *rpoE2*-F2/*rpoE2*-R2 and *chrR2*-F1/*chrR2*-R3 primer pairs (Table S1), respectively, and cloned into the two-hybrid plasmid vectors pBT and pTRG, resulting in recombinant plasmids pBT-*rpoE2* and pTRG-*chrR2*. The interaction of fusion proteins encoded in pBT-LGF2 and pTRG4 GAL11P, provided by the BacterioMatch II Two-Hybrid system, was used as positive control.

Table 1. Bacterial strains and plasmids used

Abbreviations: Ap^r, Ampicillin resistance; Cm^r, chloramphenicol resistance; Km^r, kanamycin resistance; Tc^r, tetracycline resistance.

Strain or plasmid	Relevant properties	Source or reference
Strains		
E. coli DH5α	Δ*lacU169 hsdR17 recA1 endA1 gyrA96 thiL relA1*	Gibco-BRL
E. coli S.17-1	Sm^r *recA thi pro hsdR* RP4-2(Tc::Mu; Km::Tn*7*)	Simon *et al.* (1983)
BL21λ (DE3) pLysS	*ompT hsdS*(r_B^- m_B^-) *dcm*$^+$ *endA galλ* BL21(DE3)	Novagen
A. brasilense Sp7	Wild-type strain	Nur *et al.* (1981)
chrR1::Tn*5*	*chrR1*::Tn*5* mutant of *A. brasilense* Sp7	Thirunavukkarasu *et al.* (2008)
chrR2::Km	*chrR2*::Km^r mutant of *A. brasilense* Sp7	This work
Plasmids		
pSUP202	ColE1 replicon, mobilizable plasmid, suicide vector suitable for *A. brasilense*, Ap^r, Tc^r, Cm^r	Simon *et al.* (1983)
pUC4K	Vector containing Km cassette	GE Healthcare
pGEM-T Easy	PCR product cloning vector	Promega
pTRG	Target plasmid, BacterioMatch II Two-Hybrid system	Agilent Technologies
pBT	Bait plasmid, BacterioMatch II Two-Hybrid system	Agilent Technologies
pET15b	Expression vector, Ap^r	Novagen
pMMB206	Cm^r, broad host range, low copy number, expression vector	Morales *et al.* (1991)
pBBR-MCS1-*lacZ*	Cm^r broad host range, low copy number, promoter fusion vector	Haine *et al.* (2006)
pNG2	ORF of *rpoE2–chrR2* genes from *A. brasilense* Sp7 cloned into the *Nde*I/*Bam*HI site of pET15b	This work
pNG3	Fragment A and B of the *chrR2* gene from *A. brasilense* cloned into the *Pst*I/*Eco*RI site of pSUP202	This work
pNG4	*chrR2* disruption plasmid; kanamycin resistance gene (*apt*) from pUC4K cloned into the *Bgl*II site of pNG3	This work
pMN4	*A. brasilense rpoE*1 promoter region cloned into the *Xba*I/*Pst*I site of pBBRMCS1*lacZ*	Mishra *et al.* (2008)
pNG5	*A. brasilense rpoE2* promoter region cloned into the *Xba*I/*Pst*I site of pBBRMCS1*lacZ*	This work
pNG6	*rpoE2* gene from *A. brasilense* Sp7 cloned into the *Eco*RI/*Bam*HI site of pMMB206	This work
pNG7	*chrR2* gene from *A. brasilense* Sp7 cloned into the *Eco*RI/*Bam*HI site of pMMB206	This work
pBT-*rpoE1*	*rpoE1* gene from *A. brasilense* Sp7 cloned into the *Eco*RI/*Bam*HI site of pBT	Mishra *et al.* (2011)
pBT-*rpoE2*	*rpoE2* gene from *A. brasilense* Sp7 cloned into the *Eco*RI/*Bam*HI site of pBT	This work
pTRG-*chrR2*	*chrR2* gene from *A. brasilense* Sp7 cloned into the *Eco*RI/*Xho*I site of pRTG	This work
pTRG-Gal11P	Plasmid encoding a domain (90 amino acids) of the mutant form of the Gal11 protein	Agilent Technologies
pTRG-*chrR1*	*chrR1* gene from *A. brasilense* Sp7 cloned into the *Eco*RI/*Xho*I site of pRTG	Mishra *et al.* (2011)

Protein–protein interaction was estimated by measuring β-galactosidase activity in the *E. coli* reporter strain after cotransforming it with an equal amount of pBT-*rpoE2* and pTRG-*chrR*2 expressing hybrid bait and target proteins, respectively. β-Galactosidase activity was measured twice in triplicate.

Construction of a *chrR2* null mutant in *A. brasilense* Sp7. A *chrR2* null mutant (*chrR2*::Km) of *A. brasilense* Sp7 was constructed by homologous recombination as described previously (Mishra *et al.*, 2011). Briefly, *chrR2* along with its flanking genes was amplified as two amplicons: amplicon A (1127 bp) with the primer pair *rpoE*2-AF/*chrR*2-AR and amplicon B (1125 bp) with the primer pair *chrR2*-BF/DNA Pol IV-BR (Fig. S1a, Table S1). A and B amplicons were digested with *Pst*I/*Bgl*II and *Bgl*II/*Eco*RI, respectively, and inserted between the *Pst*I and *Eco*RI sites of pSUP202 to generate pNG3. pNG3 was cleaved with *Bgl*II and ligated to a *Bam*HI digested ~1.4 kb Km^r gene cassette excised from pUC4K (GE Healthcare), to generate the *chrR2* disruption plasmid pNG4 (pSUP202:*chrR2*AKmB), which was conjugatively mobilized into *A. brasilense* Sp7 to replace the chromosomal copy of *chrR2* with *chrR*:Km to disrupt the *chrR2* gene. The Km^r and Tc^s exconjugants so obtained were analysed for allele replacement by PCR. *chrR2* was amplified with *chrR2*-specific primers using the genomic DNA of *A. brasilense* Sp7 and of the Km^r Tc^s exconjugants as templates. Whereas *A. brasilense* Sp7 produced an amplicon of approximately 654 bp showing the size of the *chrR* gene, the exconjugants produced an amplicon of approximately 2.0 kb, confirming the insertion of the Km^r gene cassette into the *chrR2* ORF (Fig. S1b). The mutant was designated *chrR2*::Km

Construction of *A. brasilense* Sp7 overexpressing RpoE2 and *chrR2*::Km overexpressing ChrR2. The genes encoding RpoE2 and ChrR2 were PCR-amplified with primer pairs *rpoE2*-F2/*rpoE2*-R2 and *chrR2*-F2/*chrR2*-R2 (Table S1), respectively, which introduced *Eco*RI–*Bam*HI and *Eco*RI–*Pst*I sites at the two ends of the amplicons.

The amplicons were digested with *Eco*RI/*Bam*HI and *Eco*RI/*Pst*I restriction enzymes and ligated with a similarly digested broad-host-range expression vector, pMMB206, having an IPTG-inducible *lacUV5* promoter. The resulting recombinant clones with *rpoE2* and *chrR2* were designated pNG6 and pNG7, respectively. The two plasmids were transformed separately into *E. coli* S17-1 and conjugatively mobilized into *A. brasilense* Sp7 and the *chrR2*::Km mutant, respectively. *A. brasilense* Sp7 (pNG6) and *chrR2*::Km (pNG7) were used to study the effects of overexpression of RpoE2 in the parent and of the complementation of the *chrR2*::Km mutant with a cloned copy of *chrR2*, respectively.

Estimation of carotenoids. Overnight cultures of *A. brasilense* Sp7, *A. brasilense* Sp7 (pNG6, *rpoE2* cloned in pMMB206), the *chrR2*::Km mutant and *chrR2*::Km (pNG7, *chrR2* cloned in pMMB206) were grown to stationary phase with shaking at 175 r.p.m. at 30 °C in LB broth with the respective antibiotics and IPTG, if required. Carotenoid content and UV–visible absorption spectra were determined spectrophotometrically as described previously (Thirunavukkarasu *et al.*, 2008). Carotenoids were estimated three times, with each strain analysed in triplicate.

Measurement of sensitivity to reactive oxygen species and antibiotics. Overnight cultures of *A. brasilense* Sp7, *A. brasilense* Sp7 (pNG6), the *chrR2*::Km mutant and *chrR2*::Km (pNG7) were grown to the late exponential phase in LB medium at 30 °C with the respective antibiotics. The preculture (100 µl) of each strain was mixed with 5 ml 0.5 % top agar supplemented with 1 mM IPTG, poured on top of LB agar plates (1.5 % agar) and allowed to solidify. Sterile filter disks (diameter 10 mm; HiMedia) were soaked with 50 µl 10 mM paraquat, 5 mM methylene blue, 5 mM toluidine blue, 5 % hydrogen peroxide, 50 mM cumene hydroperoxide and 100 mM cadmium chloride. Similarly, disks containing nalidixic acid (30 µg per disk), aztreonam (30 µg per disk), cefixime (5 µg per disk) and cefotaxime (30 µg per disk) were placed on the top of the agar. The diameters of the inhibition zones surrounding the impregnated disks were measured after 2 days of incubation at 30 °C. Each experiment was done in triplicate and repeated at least three times.

Proteome analysis by 2D gel electrophoresis. Mid-exponential phase cells of *A. brasilense* Sp7, the *chrR2*::Km mutant and *A. brasilense* Sp7 (pNG6), overexpressing RpoE2, were harvested by centrifugation, and the pellet was washed twice with 20 mM Tris/HCl (pH 8.0) and resuspended in 1.5 ml 2D lysis buffer (20 mM Tris/HCl, 4 % CHAPS and 1 mM PMSF). The resulting cell suspension was vortexed for 15 min followed by brief sonication (three pulses of 10 s) on ice. The resulting lysate was centrifuged at 10 000 ***g*** for 20 min at 4 °C to separate the dissolved proteins in the supernatant from the cell debris. The supernatant containing the soluble protein fraction was collected and treated with RNase A (Genie) and DNase I (New England Biolabs) for 1 h to remove nucleic acids. A total of 1.5 mg soluble proteins was precipitated with four volumes of chilled acetone and washed twice with chilled acetone. Protein pellets were air-dried for 15 min and then solubilized by vigorous vortexing in 250 µl rehydration buffer [8 M urea, 2 % CHAPS, 0.5 % ampholytes of isoelectic point (pI) range 4–7 and 2 mM DTT]. Solubilized proteins were poured into a rehydration tray and incubated with IPG strips (13 cm; pH range 4–7) (GE Healthcare) for 1 h to absorb the sample onto the strip gel material. After 1 h, the strips were removed from the rehydration tray and placed into the focusing tray for active rehydration and focusing. The program used for IEF was as follows: step 1, 20 V for 12 h; step 2, gradient to 500 V for 1 h; step 3, 500 V for 1 h; step 4, gradient to 8000 V for 4 h; and step 5 8000 V for 35 000 Vh. After the IEF, the IPG strips were equilibrated by first incubating them in an equilibration solution (6 M urea, 0.375 M Tris/HCl, pH 8.8, 2 % SDS, 20 % glycerol and 2 % DTT), followed by incubation in 200 mM iodoacetamide in the same equilibration solution instead of 2 % DTT for 15 min each to reduce and modify the cysteine residues. Equilibrated strips were briefly dipped into a graduated cylinder containing 1 × TGS (0.192 M glycine, 25 mM Tris and 0.1 % SDS) running buffer. The second-dimension SDS-PAGE was then run in a cooling apparatus (GE Healthcare). After the electrophoresis, gels were stained with colloidal Coomassie brilliant blue dye (G250) overnight and destained to visualize the protein spots. ImageMaster 2D Platinum 7 software (GE Healthcare) was used to identify the differentially expressed proteins observed in three independent biological samples with two replicates each using the statistics available in the software. Finally, the selected spots were processed for in-gel trypsin digestion and the eluted peptides submitted for MALDI-TOF/TOF analysis. The peptide mass list obtained from the analyser (Bruker Daltonics) was used for a MASCOT search against the NCBI database. A peptide mass tolerance of ±1.2 Da and an MS/MS tolerance of ±0.6 Da were set, and only one missed cleavage was allowed. Carbamidomethylation (C) as a fixed modification and oxidation (M) as a variable modification were considered. A probability score of $P<0.05$ was used as a criterion for identification.

Construction of an *rpoE2* promoter–*lacZ* fusion. For the construction of a translational fusion of the *rpoE2* promoter with a promoterless *lacZ* gene, the 503 bp region located upstream of *rpoE2* was PCR-amplified using the *rpoE2*-FPr/*rpoE2*-RPr primer pair (Table S1). The amplicon was cloned into the *Xba*I–*Pst*I site of the pBBR-MCS-*lacZ* vector to generate pNG5, which was conjugatively mobilized in *A. brasilense* strains via *E. coli* S17-1.

***β*-Galactosidase assay.** *A. brasilense* Sp7, *chrR1*::Tn*5* (Mishra *et al.*, 2008) and *chrR2*::Km mutants harbouring pNG5, pMN4 (*rpoE1–lacZ* fusion) or the vector, pBBR-MCS-lacZ, were grown in MMAB with or without different stresses by supplementing the mid-exponential phase cultures with 10 µM methylene blue, 1 µM toluidine blue and 1 µM paraquat, and were grown for another 2 h. *β*-Galactosidase assays (Miller, 1972) were performed twice in triplicate using 1.5 ml culture of equalized OD_{600}.

RESULTS

The *A. brasilense* Sp245 genome harbours two pairs of σ^E and ChrR

A BLAST search of the 7.5 Mb genome sequence of *A. brasilense* Sp245 (http://genome.ornl.gov/microbial/abra/19sep08) using a deduced amino acid sequence of RpoE of *E. coli* as the query revealed the presence of nine RpoE paralogues. When the genes flanking *rpoE* were analysed, five *rpoE* paralogues were accompanied by a downstream gene predicted to be an anti-sigma factor, whereas four *rpoE* paralogues did not contain any gene encoding an anti-sigma factor-like protein. Furthermore, BLAST analysis of the amino acid sequence of the five anti-sigma factors showed two of them to be homologous to the ZAS factors (Paget *et al.*, 2001). Both of these anti-sigmas showed very high similarity to ChrR, a ZAS-family anti-sigma factor from *R. sphaeroides* (Anthony *et al.*, 2004; Newman *et al.*, 2001), and hence are designated ChrR1 and ChrR2. The genes encoding the earlier described pair of σ^E/anti-σ^E (Mishra *et al.*, 2011; Thirunavukkarasu *et al.*, 2008) are redesignated now as *rpoE1* and *chrR1*. Consequently, the genes encoding the second pair of σ^E and ChrR are designated *rpoE2* and *chrR2*.

ChrR2 is homologous to ChrR1 and ChrR

ChrR2 showed striking sequence similarity to ChrR1 of *A. brasilense* Sp7 and ChrR of *R. sphaeroides* (Fig. S2). Both ChrR2 and ChrR1 possess the conserved His6, His32, Cys36 and Cys39 residues that are involved in the binding of a zinc atom in the ASD, and His141, His143, Glu147 and His177 residues which are involved in the binding of another zinc atom in the cupin-like domain (CLD). The ChrR protein of *Caulobacter crescentus* also possesses the conserved zinc-binding amino acid residues in the CLD although it lacks the typical zinc-binding motif (HxxxCxxC) that is present in the ASD of other ChrR proteins. All four ChrR proteins also contained the conserved cysteine residues at positions equivalent to 187 and 189. In comparison with the four cysteine residues of *R. sphaeroides* ChrR, the ChrR1 and ChrR2 proteins contain eight and six cysteine residues, respectively.

rpoE2 and *chrR2* are cotranscribed

The gene encoding ChrR2, like many other anti-sigma factor genes, is also located downstream of *rpoE2* in the genome of *A. brasilense* Sp245 (Fig. 1a). In order to understand whether there is any difference in the organization of *rpoE2–chrR2* between *A. brasilense* Sp245 and *A. brasilense* Sp7, we determined the nucleotide sequence of the *rpoE2–chrR2* gene region of *A. brasilense* Sp7 and compared it with that of Sp245, and it showed 97 % identity with its homologues in *A. brasilense* Sp245. Although the start codon (GUG) of *chrR2* and the stop codon (UGA) of *rpoE2* showed an overlap (GUGA) in *A. brasilense* Sp245, *A. brasilense* Sp7 showed a space of two nucleotides (CC) between the start codon (GUG) of *chrR2* and the stop codon (UGA) of *rpoE2*. Such a tight organization of the two genes suggested that they might be cotranscribed. RT-PCR analysis revealed that the primers specific for *rpoE2* and *chrR2* produced the expected amplicons of approximately 543 and approximately 654 bp, respectively (Fig. 1b, Table S1). The transcriptional organization of *rpoE2* and *chrR2* was analysed by RT-PCR with the total RNA isolated from *A. brasilense* Sp7, and showed that the *rpoE2*-F/*chrR2*-R primers produced an expected amplicon of approximately 1.2 kb (Fig. 1c), and primers *rpoE2*-F/*chrR2*-RI (complementary to nucleotides 230–247 of *chrR2*) also generated an amplicon of the expected size (769 bp). Examination of both these amplicons indicated that *rpoE2* and *chrR2* constitute a single transcriptional unit. The absence of any amplicon in a PCR without reverse transcriptase showed that the RNA preparation was free of contamination from genomic DNA.

Mapping the TSS of *rpoE2*

In order to identify the promoter elements of the *rpoE2–chrR2* operon, 5′ RACE was carried out with the total RNA

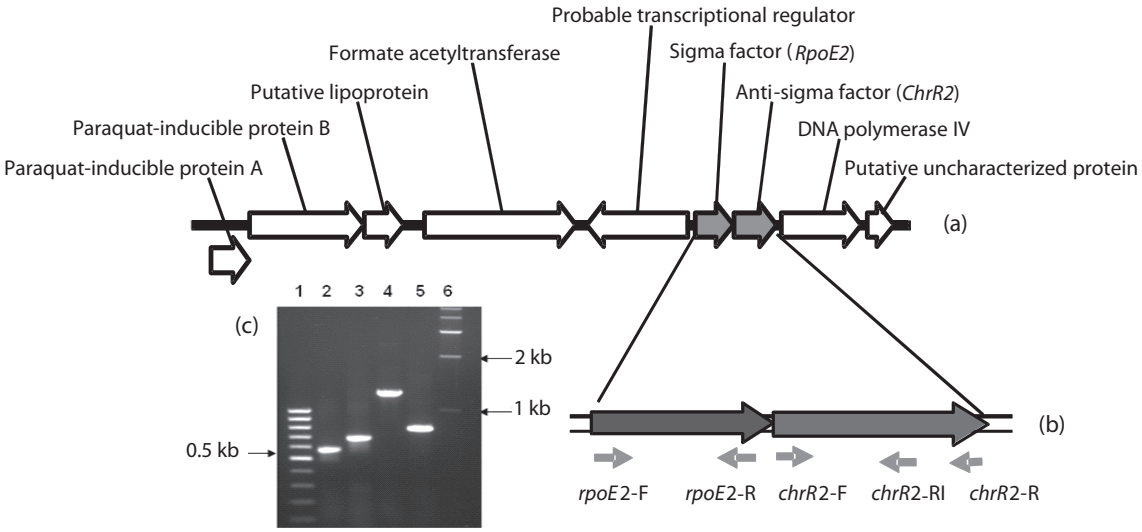

Fig. 1. (a) Organization of *rpoE2–chrR2* and other neighbouring genes in *A. brasilense* Sp7. Arrows indicate the orientation of genes present on the + or − DNA strand. Downstream of the gene encoding ChrR2, there was an ORF encoding DNA damage-inducible DNA polymerase IV (DinP). Upstream of *rpoE2*, a gene encoding a transcriptional regulator was located. The genes encoding formate acetyltransferase, a putative lipoprotein and paraquat-inducible proteins (PqiA and PqiB) were present further upstream of the transcriptional regulator. (b) Location of the primers used for RT-PCR amplification of *rpoE2*, *chrR2* and *rpoE2chrR2* with a total RNA sample isolated from *A. brasilense* Sp7. (c) Agarose gel showing amplicons obtained with *rpoE2*-specific (*rpoE2*-F/*rpoE2*-R) primers (lane 2), *chrR2*-specific (*chrR2*-F/*chrR2*-R) primers (lane 3), with *rpoE2* forward (*rpoE2*-F) and *chrR2* reverse (*chrR2*-R) primers (lane 4), and cotranscription of the *rpoE2chrR2* gene with *rpoE2* forward (*rpoE2*-F) and *chrR2* reverse (*chrR2*-RI) primers designed from the internal sequence of the *chrR2* ORF (lane 5); lanes 1 and 6 show the bands of 100 bp and 1 kb DNA ladders (NEB).

of *A. brasilense* Sp7 cells to determine the TSS. Sequencing of amplified products revealed a single TSS corresponding to an adenine (A) located 89 bp upstream of the *rpoE2* start codon (Fig. S3a). An analysis of the region upstream of the identified TSS revealed that a −10 element (CCCCTA) was located 6 bp upstream of the TSS and was at a distance of 15 bp from the −35 element (GAATCC) (Fig. S3b). A comparison of the promoter sequence of Abr *rpoE2* with that of Abr *rpoE1* and Rsp *rpoE* revealed that the 'ATCC' motif in the −35 element and 'TA' motif in the −10 element were conserved (Fig. S3c). We also compared the 2.3–2.4 and 4.2 regions of AbrRpoE1 and AbrRpoE2 with that of Rsp RpoE, which are known to recognize −10 and −35 elements, respectively (Fig. S3d). Whereas the 2.3–2.4 regions of AbrRpoE1 and AbrRpoE2 showed more identity with each other, region 4.2 of AbrRpoE2 had higher identity with RspRpoE than with AbrRpoE1. The four critical residues of RspRpoE region 4.2 predicted to contact the −35 element were identical to those present in AbrRpoE1. However, one of these four critical residues, serine (S), was replaced by a threonine (T) in RpoE2.

ChrR2 and RpoE2 proteins physically interact with each other

Whether RpoE2 and ChrR2 physically interact with each other was analysed by an *E. coli* two-hybrid assay as well as by a pull-down assay. The BacterioMatch II Two-Hybrid system using *E. coli* as a host (Kumar *et al.*, 2009) showed that the transformants carrying the two recombinant plasmids, one expressing RpoE2 and the other expressing ChrR2, displayed a $LacZ^+$ phenotype and produced blue colonies on X-Gal plates, indicating a positive interaction between the two proteins. A quantitative *β*-galactosidase assay of the cotransformants also showed that the strength of the *in vivo* interaction between RpoE2 and ChrR2 was almost as great as that observed in the positive control (Fig. 2a). The interaction was considerably lower in the negative control harbouring pBT and pTRG-*chrR*2. These analyses revealed that ChrR2 is able to physically interact with RpoE2.

Results of the two-hybrid assay between RpoE2 and ChrR2 were further validated by an *in vitro* tag-based pull-down assay. The tight organization of the start codon of *chrR2* and the stop codon of *rpoE2* shows not only cotranscription of the two genes but also synthesis of the two proteins by translational coupling, a mechanism which ensures the synthesis of interacting proteins in stoichiometric proportions (Norman *et al.*, 2000; Mishra *et al.*, 2011). In order to avoid problems resulting from the unequal solubility and stability of the two interacting partner proteins when overexpressed separately (Thakur *et al.*, 2010), we cloned both genes, *rpoE2* and *chrR2*, together in pET15b (pNG2) to coexpress 6 × His-RpoE2 from the Shine–Dalgarno (SD) sequence of the vector and the wild-type ChrR2 from its native SD sequence located at the 3′ end of the *rpoE2*. Thus, the expected size of RpoE2 protein along with the 6 × His tag

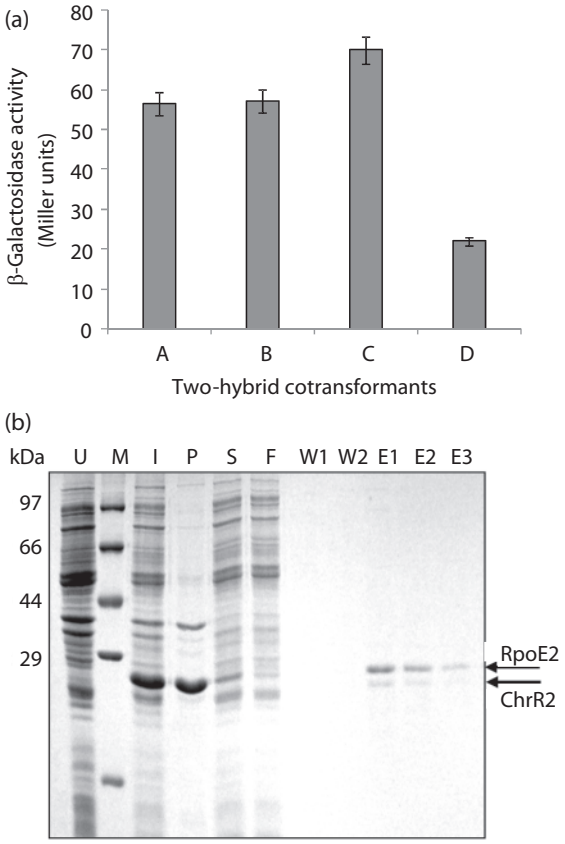

Fig. 2. (a) *β*-Galactosidase activity of the BacterioMatch Two-Hybrid system cotransformed with pBT-*rpoE1*/pTRG-*chrR1* (A) and pBT-*rpoE2*/pTRG-*chrR2* (B), showing the protein–protein interaction between RpoE1/ChrR1 and RpoE2/ChrR2 of *A. brasilense* Sp7, respectively. pBT-LGF2/pTRG-GAL11P (C) and pBT/pTRG-*chrR2* (D) were used as positive and negative controls, respectively. (b) SDS-PAGE showing proteins in the soluble extracts of *E. coli* BL21*λ* (DE3) pLysS harbouring pNG3 (U, uninduced crude cell lysate; I, induced; P, pellet fraction of His-tagged fusion protein; S, soluble fraction; F, flow through; W1, W2, wash; E1, E2, E3, purified eluted proteins). Lanes E1–E3 show that ChrR2 co-purified with His–RpoE2 after passing the soluble extract from *E. coli* cells coexpressing His–RpoE2 and ChrR2 over Ni-NTA agarose under non-denaturing conditions. Lane M, protein molecular mass marker.

and of wild-type ChrR2 proteins should be 22 and 23.8 kDa, respectively. Since only 6 × His-RpoE2 could bind directly to the Ni-NTA agarose when the soluble extract from *E. coli* cells expressing both 6 × His-RpoE2 and wild-type ChrR2 was passed over the Ni-NTA agarose column, the presence of ChrR2 along with 6 × His-RpoE2 in the eluted fraction indicated that ChrR2 formed a complex with RpoE2 (Fig. 2b). The identity of both the eluted proteins was further confirmed as an ECF sigma factor and an anti-sigma factor by MALDI-MS/MS (Fig. S4). These observations strongly suggested that ChrR2 physically interacts with RpoE2 by forming a RpoE2–ChrR2 complex.

Effect of inactivation of *chrR2* or overexpression of *rpoE2* on *A. brasilense*

The obvious phenotypic difference among *A. brasilense* Sp7, *chrR2*::Km mutant and *A. brasilense* Sp7 (pNG6), which overexpresses *rpoE2*, was the orange-red colour of the colonies of the *chrR2*::Km mutant and *A. brasilense* Sp7 (pNG6), and the creamish-white colour of the *A. brasilense* Sp7 colonies on LB agar plates (Fig. 3a). The amount of carotenoids produced by the *chrR2*::Km mutant, however, was significantly lower than that of the previously isolated *chrR1*::Tn*5* mutant (Thirunavukkarasu *et al.*, 2008; data not shown). Absorption spectra of the methanolic extracts of the stationary phase cultures of *A. brasilense* Sp7, *A. brasilense* Sp7 (pNG6) and the *chrR2*::Km mutant showed carotenoid-specific peaks at 485 nm. *A. brasilense* Sp7 (pNG6) produced more carotenoids than the *chrR2*::Km mutant, whereas *A. brasilense* Sp7 produced the least amount of carotenoids (Fig. 3b). Quantitative estimation of carotenoids also showed that expression of a wild-type copy of the *chrR2* gene in the *chrR2*::Km mutant restored the wild-type levels of carotenoids, whereas expression of the *rpoE2* gene in the parent and *chrR2*::Km mutant resulted in the overproduction of carotenoids (Fig. 3c). There was no increase in carotenoid content in *A. brasilense* Sp7 and *chrR2*::Km harbouring pMMB206.

Since carotenoids are known to scavenge $^1O_2$, and disruption of *chrR2* or overexpression of *rpoE2* in *A. brasilense* Sp7 results in the overproduction of carotenoids, it was assumed that RpoE2–ChrR2 might confer tolerance to photooxidative stress in *A. brasilense* Sp7. We tested the effect of different oxidative stress-causing agents, i.e. paraquat (superoxide), methylene blue plus light ($^1O_2$), toluidine blue plus light ($^1O_2$ and superoxide), hydrogen peroxide, cumene hydroperoxide (peroxide) and cadmium (heavy metal) on the growth of *A. brasilense* Sp7, *A. brasilense* Sp7 (pNG6), the *chrR2*::Km mutant and *chrR2*::Km (pNG7), the complemented strain. Inactivation of *chrR2* or overexpression of *rpoE2* in *A. brasilense* Sp7 conferred notable tolerance to methylene blue and paraquat (Fig. 4a). It also conferred some tolerance to toluidine blue. The expression of a wild-type copy of the *chrR2* gene in the *chrR2*::Km mutant rendered the mutant almost as sensitive as the wild-type, indicating complementation. However, *A. brasilense* Sp7, *A. brasilense* Sp7 (pNG6) and the *chrR2*::Km mutant did not show any notable difference in their sensitivity to other stress agents such as hydrogen peroxide, cumene hydroperoxide or cadmium chloride.

When we compared *A. brasilense* Sp7, the *chrR2*::Km mutant and *A. brasilense* Sp7 overexpressing *rpoE2* for their sensitivity to antibiotics, we found that *chrR2* disruption or *rpoE2* overexpression conferred on *A. brasilense* Sp7 resistance to aztreonam, cefixime and cefotaxime, which are known to affect the strength of the cell wall by inhibiting mucopeptide synthesis (Fig. 4b). It also conferred some resistance to nalidixic acid, a quinolone antibiotic that inhibits DNA gyrase activity. Complementation of the *chrR2*::Km mutant with the cloned copy of *chrR2* restored the antibiotic sensitivity to wild-type levels.

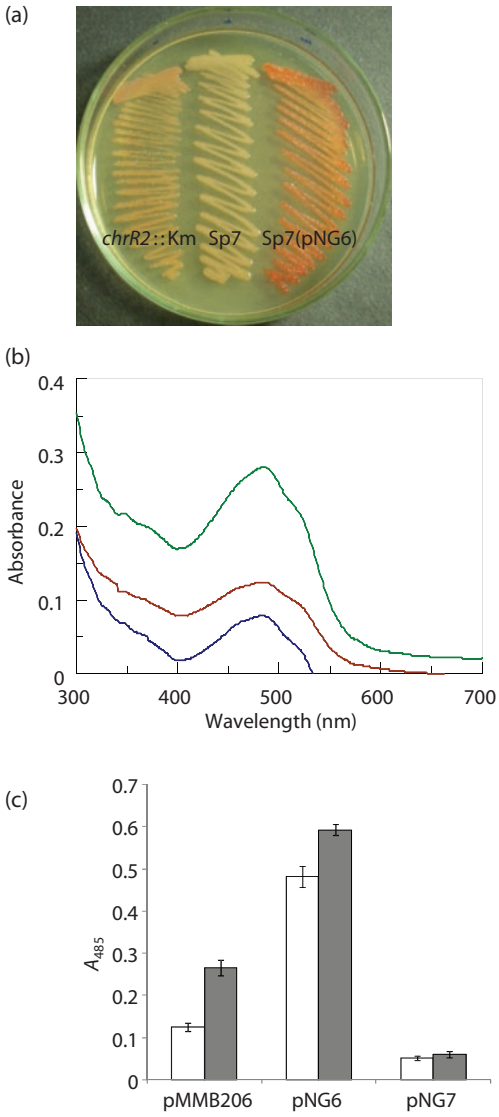

Fig. 3. (a) LB agar plate showing differences in carotenoid content of *A. brasilense* Sp7, *A. brasilense* Sp7 (pNG6) and the *chrR2*::Km mutant. (b) Absorption spectra of methanolic extracts of *A. brasilense* Sp7, *A. brasilense* Sp7 (pNG6) and the *chrR2*::Km mutant (green, *A. brasilense* Sp7 (pNG6); brown, *chrR2*::Km; blue, *A. brasilense* Sp7). (c). Effect of *rpoE*2 and *chrR*2 expression on carotenoid content in *A. brasilense* Sp7 (white bars) and the *chrR2*::Km mutant (grey bars). Carotenoid content was determined by measuring the A_{485} of methanol extracts prepared from stationary phase cultures grown as described in Methods. Error bars, SD from three replicates of two independent experiments.

Regulation of *rpoE2* promoter activity

In view of the earlier observations that most of the *rpoE* promoters are autoregulated, the *rpoE2–lacZ* fusion

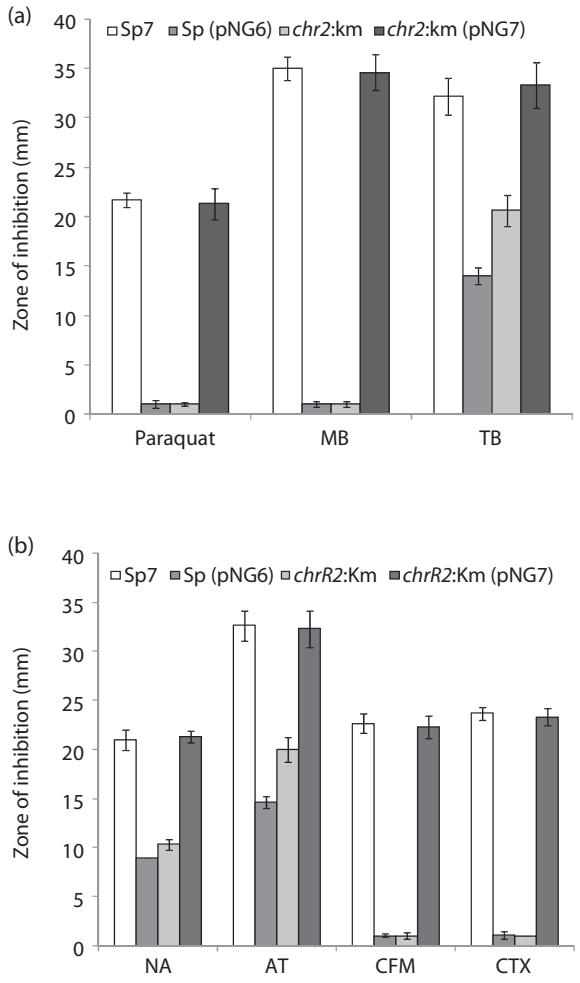

Fig. 4. Comparison of the sensitivity of *A. brasilense* Sp7, Sp7 (pNG6), the *chrR2*::Km mutant and complemented *chrR2*::Km (pNG7) strains to oxidative stress agents and antibiotics by disk diffusion assay. (a) Sensitivity to 10 mM paraquat, 5 mM methylene blue and 5 mM toluidine blue. (b) Sensitivity to 30 μg nalidixic acid (NA), 30 μg aztreonam (AT), 5 μg cefixime (CFM) and 30 μg cefotaxime (CTX). Each bar represents the mean diameter of the zone of inhibition measured in at least three independent assays performed in triplicate. Error bars, SD. The zone of inhibition is expressed as the total diameter of the clear zone minus the diameter of the filter disk.

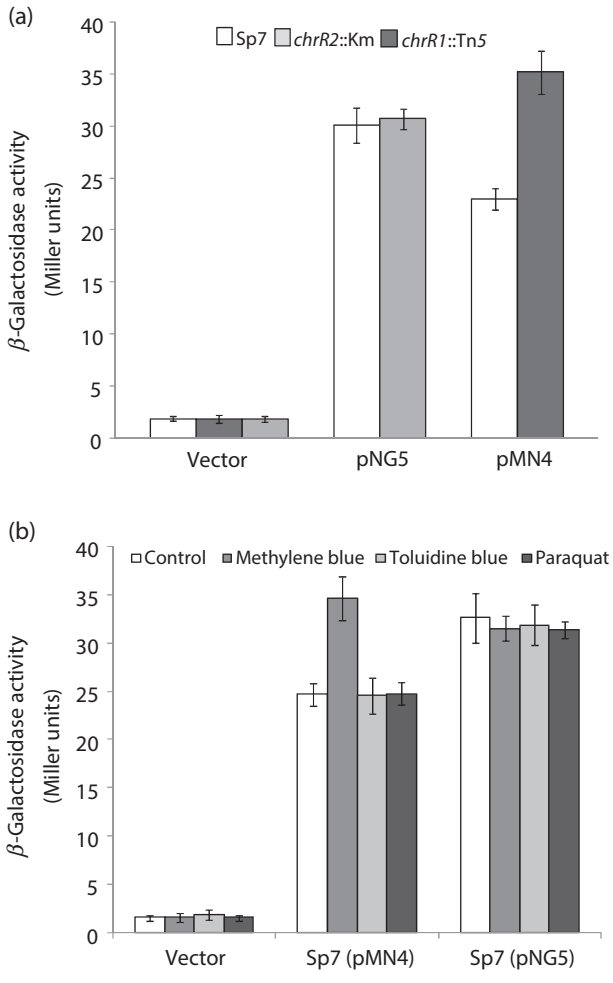

Fig. 5. (a) β-Galactosidase activities of mid-exponential phase cells of *A. brasilense* Sp7, the *chrR2*::Km mutant harbouring an *rpoE2–lacZ* fusion plasmid, pNG5, and the *chrR1*::Tn*5* mutant harbouring an *rpoE1–lacZ* fusion plasmid, pMN4. The vector (pBBR-MCS-*lacZ*) was used as a control. (b) Effect of methylene blue (10 μM), toluidine blue (1 μM) and paraquat (1 μM) on the β-galactosidase activity of *A. brasilense* Sp7 cells harbouring an *rpoE1–lacZ* fusion (pMN4) and an *rpoE2–lacZ* (pNG5) fusion. Assays were performed twice in triplicate; error bars, SD.

plasmid (pNG5) was mobilized into *A. brasilense* Sp7 and the *chrR2*::Km mutant. The activity of the *rpoE2* promoter, as reflected in the β-galactosidase activity, was almost the same in the parent as in the *chrR2*::Km mutant, indicating that the *rpoE2* promoter was not autoregulated (Fig. 5a). On the other hand, expression of the *rpoE1–lacZ* fusion (pMN4) in the *chrR1*::Tn5 mutant and in *A. brasilense* Sp7 showed a significantly higher β-galactosidase activity in the mutant, indicating the RpoE1-dependence of the *rpoE1*P2 promoter. We also observed that under stress-free conditions the activity of the *rpoE2* promoter in *A. brasilense* Sp7 was 35–40 % greater than that of the *rpoE1* promoter. Treatment with methylene blue, paraquat and toluidine blue did not lead to any notable difference in the activity of the *rpoE2* promoter. However, *rpoE1* promoter activity in *A. brasilense* Sp7 was significantly induced by methylene blue in the presence of light (Fig. 5b).

Identification of differentially expressed proteins in *A. brasilense* Sp7 overexpressing *rpoE2*

Since the expression of ECF sigma factor-controlled genes is prevented by the binding of an ECF sigma factor with its

cognate anti-sigma factor, inactivation of the anti-sigma factor is expected to release the ECF sigma factor to drive the expression of its target genes. Thus, a comparison of the proteomes of *A. brasilense* Sp7, *chrR2*::Km mutant and *A. brasilense* Sp7 overexpressing *rpoE2* in 2D gels and identification of the differentially expressed proteins was expected to reveal the genes/proteins controlled by RpoE2–ChrR2. Such a comparison of the 2D gels showed several proteins that were upregulated slightly in the *chrR2*::Km mutant and more pronouncedly in *A. brasilense* Sp7 overexpressing *rpoE2*. Therefore, we identified a total of 25 upregulated proteins in *A. brasilense* Sp7 overexpressing *rpoE2* by MS (Table 2, Fig. S5). The proteins that were upregulated by $\geqslant$2.0-fold included alkyl hydroperoxide reductase (AZOBR_p1130169), ATP-dependent Clp protease (AZOBR_p1180006), chaperonin GroEL (AZOBR_20016), methionine ABC transporter periplasmic-binding component (AZOBR_p1120011), molybdenum ABC transporter (AZOBR_p1150017), fasciclin domain hypothetical protein (AZOBR_140066), GTP cyclohydrolase I (AZOBR_10090), acetyl-CoA acetyltransferase with thiolase domain (AZOBR_p440018), glyceraldehyde-3-phosphate dehydrogenase (AZOBR_150011), 50S ribosomal protein L9 (AZOBR_110102), adenylosuccinate synthase (AZOBR_150079), single-stranded DNA-binding protein (AZOBR_p120080), ATP synthase alpha subunit (AZOBR_40304) and an extracellular ligand-binding protein receptor (AZOBR_p280033). The proteins that were upregulated by 1.5- to <2.0-fold included chaperonin GroES (AZOBR_20015), elongation factor Tu (AZOBR_160001), elongation factor G (AZOBR_150110), cold shock protein (AZOBR_p1130129), cobaltochelatase CobS subunit (AZOBR_40113), glutamine synthetase (AZOBR_100228), conserved exported protein (AZOBR_p460010), UTP-glucose-1-phosphate uridylyltransferase (AZOBR_p440128), endoribonuclease L-PSP (AZOBR_150112), ketol acid reductoisomerase (AZOBR_100112) and a conserved protein of unknown function (AZOBR_10054).

Identification of a putative RpoE2-dependent promoter consensus

The genes encoding upregulated proteins in *A. brasilense* Sp7 overexpressing *rpoE2* are expected to be regulated by RpoE2 directly or indirectly. To test whether DNA sequences upstream of the upregulated genes/operons contain a common sequence element we searched for a conserved motif using BioProspector (Liu *et al.*, 2001). Of the 17 proteins showing a twofold or greater increase in abundance in response to mutation of *chrR2* or overexpression of *rpoE2*, 14 were encoded by genes located downstream of a conserved motif in their predicted promoter region. This motif contains two conserved sequences, G/CAA and C/GTTC, separated by a spacer region of 17–19 nt (Fig. 6), which is similar to the −35 and −10 regions of the ECF12, ECF15 and ECF 27 type group IV bacterial sigma factors (Staroń *et al.*, 2009).

DISCUSSION

This report highlights some unique features of the rhizobacterium *A. brasilense* Sp7 for responding to photooxidative stress. Previously, we had shown that a pair of σ^E–ChrR in *A. brasilense* Sp7 was involved in controlling its response to photooxidative stress by synthesizing carotenoids. In this report we have shown that *A. brasilense* Sp7 harbours an additional pair of σ^E–ChrR which is also involved in conferring tolerance to photooxidative stress via carotenoid synthesis and some additional pathways. Although the targets of σ^E in a large number of bacteria include proteins that define a set of functions needed for their response to $^1O_2$, none of them were shown to have any carotenoid biosynthetic genes as member of σ^E–ChrR regulons (Dufour *et al.*, 2008). A similar redundancy of functions has been shown earlier in *R. sphaeroides*, in which the alternative sigma factors RpoH1 and RpoH2 were both involved in the $^1O_2$ response and in the heat stress response, but the former played the major role in the heat stress response and the latter was mainly involved in the $^1O_2$ response (Nuss *et al.*, 2010). To cope with photooxidative stress a cell requires the synthesis of macromolecules that can prevent damage by scavenging $^1O_2$ and which can repair the cellular damage by refolding the misfolded proteins, replacing damaged proteins by new synthesis, and repairing DNA by replacing damaged nucleosides such as 8-oxo-7,8-dihydro-2′-deoxyguanosine with 2′-deoxyguanosine (Ravanat *et al.*, 2004). In contrast to most other bacteria, *A. brasilense* prevents and minimizes the damage by synthesizing carotenoids, which are known to scavenge $^1O_2$ (Cogdell *et al.*, 2000; Glaeser & Klug, 2005)

Members of the α-proteobacteria such as *R. sphaeroides* and *Caulobacter crescentus* respond to photooxidative stress by inactivation of a ChrR-type anti-sigma factor which, under reducing cytosolic conditions, keeps the cognate ECF sigma factor sequestered and hence unavailable for initiation of transcription from its target promoters (Anthony *et al.*, 2004; Lourenço & Gomes, 2009). Here, we have shown that like most other ECF sigma factors, *rpoE2* and *chrR2* are cotranscribed, and that their products physically interact with each other, but that they show a lack of autoregulation. The $^1O_2$-mediated dissociation of the RpoE2–ChrR2 complex and consequent release of RpoE2 provides a rapid mechanism to cope with oxidative stress. The RpoE1–ChrR1 complex, on the other hand, provides *A. brasilense* with a mechanism to adapt to oxidative stress involving autoregulation to induce the expression of RpoE1 as well as its target genes (Mishra *et al.*, 2011).

Although the role and regulation of ChrR-type ZAS factors have been described in detail for *R. sphaeroides* (Anthony *et al.*, 2004) and *C. crescentus* (Lourenço & Gomes, 2009), there is no report, to our knowledge, on the occurrence, role and regulation of two zinc anti-sigma factors in any other species of Gram-negative bacteria. Both the ChrR paralogues from *A. brasilense* contain an N-terminal ASD and a C-terminal CLD, and are homologous to the ChrR of

Table 2. Identification of differentially expressed proteins in the *chrR2*::Km mutant and *A. brasilense* Sp7 overexpressing *rpoE2*

Spot no.	Accession no.	Matched locus tag	Protein identified	Probable function	Mascot score	No. of peptides matched	Hypothetical molecular mass (Da)/pI	Fold change*	Coefficient of variation
Proteins upregulated in the *chrR2*::Km mutant and in *A. brasilense* Sp7 overexpressing RpoE2									
1	gil392382348	AZOBR_110102	RplI	50S ribosomal protein L9	407	11	20 689/5.17	3.0	0.36
2	gil392378525	AZOBR_p1130169	AhpC	Alkyl hydroperoxide reductase, C subunit	247	7	20 794/5.13	2.4	0.32
3	gil392378874	AZOBR_p1180006	ClpP	ATP-dependent Clp protease proteolytic subunit	489	11	23 308/5.73	2.4	0.34
4	gil392378708	AZOBR_p1150017	ModA	Molybdenum ABC transporter	615	10	26 103/6.76	2.1	0.29
5	gil392381055	AZOBR_20016	GroEL	Large subunit of chaperonin GroESL	619	29	57 795/5.02	2.0	0.10
6	gil392378305	AZOBR_p1120011	NlpA	Methionine ABC transporter, periplasmic-binding component	388	8	28 512/6.18	2.0	0.05
7	gil356877838	AZOBR_150110	FusA	Elongation factor G	541	11	79 129/5.11	1.8	0.09
8	gil392381222	AZOBR_40113	CobS	Cobaltochelatase, CobS subunit	458	18	37 542/5.40	1.8	0.05
9	gil392383014	AZOBR_160001	TufB1	Elongation factor Tu (EF-Tu)	578	24	43 319/5.42	1.5	0.05
Proteins upregulated only in *A. brasilense* Sp7 overexpressing RpoE2									
10	gil392382531	AZOBR_140066	COG2335	Conserved hypothetical protein; Beta-Ig-H3/Fasciclin domain	261	3	16 634/6.5	61.0	0.25
11	gil392380603	AZOBR_10090	FolE	GTP cyclohydrolase I	401	12	24 530/6.25	7.0	0.50
12	gil392379932	AZOBR_p440018	PhbA	Acetyl-CoA acetyltransferase with thiolase domain	331	11	40 666/6.41	3.5	0.55
13	gil392382782	AZOBR_150011	GapB	Glyceraldehyde-3-phosphate dehydrogenase	503	13	36 364/7.18	2.5	0.4
14	gil356877809	AZOBR_150079	PurA	Adenylosuccinate synthase	403	11	46 544/5.77	2.5	0.1
15	gil392377389	AZOBR_p120080	Ssb	Single-stranded DNA-binding protein	202	8	16 547/5.55	2.0	0.05
16	gil356876370	AZOBR_40304	AtpA	ATP synthase alpha subunit	288	9	55 127/6.31	2.0	0.1
17	gil356881167	AZOBR_p280033	LivK	Extracellular ligand-binding protein receptor	885	12	39 835/6.17	2.0	0.15
18	gil392382076	AZOBR_100228	GlnA	Glutamine synthetase	221	11	52 270/5.19	1.5	0.14
19	gil392380120	AZOBR_p460010	COG3181	Conserved exported protein of unknown function	601	10	33 823/6.93	1.5	0.11
20	gil392380036	AZOBR_p440128	GalU	UTP-glucose-1-phosphate uridylyltransferase	450	8	32 486/5.94	1.5	0.10
21	gil392381054	AZOBR_20015	GroES	Small subunit of chaperonin GroESL	238	5	10 443/5.84	1.5	0.1
22	gil392382875	AZOBR_150112	TdcF	Putative endoribonuclease L-PSP	231	4	12 483/5.23	1.5	0.15
23	gil356875531	AZOBR_10054	COG4223	Conserved protein of unknown function	50	1	65 196/4.87	1.5	0.13
24	gil288959011	AZOBR_100112	Ilvc	Ketol acid reductoisomerase	288	8	37 512/6.03	1.5	0.1
25	gil392378485	AZOBR_p1130129	CspC	Putative cold shock protein	369	9	20 430/6.42	1.4	0.05

*Fold difference was calculated by comparing with the quantity of each protein in *A. brasilense* Sp7 using Imagemaster 2D Platinum 7 (GE Healthcare).

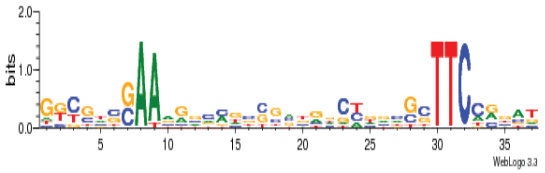

	-35	-10
folE	GGGCCG**GAA**CCGGC-N_{09}-ATGGC**TTC**CCGGT-N_{124}-**ATG**
rplI	GCGCAG**GAA**TCGTC-N_{08}-CGTGT**TTC**CGCTT-N_{144}-**ATG**
ahpC	ATCGAT**CAA**AGCGA-N_{09}-TTCGC**TTC**CATCG-N_{176}-**ATG**
clpP	ATTGTG**CAA**AGGGC-N_{08}-TCTCC**TTC**CCGAT-N_{213}-**ATG**
modA	CGCGCC**GAT**ATTCC-N_{09}-GACGA**TTC**TGTCA-N_{072}-**ATG**
groES	GGCAGG**CAA**CAAAA-N_{08}-TCTTT**TTC**AATGC-N_{173}-**ATG**
FusA	TGCTTC**GAA**AAAAT-N_{10}-TGACC**TTC**CGGAT-N_{119}-**ATG**
nlpA	GTCCTT**CAA**GGACC-N_{09}-AGACC**TTC**CGCAA-N_{140}-**GTG**
phbA	TTTCAA**GAA**GGGTC-N_{09}-GAATG**TTC**AGAT-N_{425}-**GTG**
gapB	GTCGTC**GAA**AGTCA-N_{09}-GGCGG**TTC**CGTTT-N_{308}-**ATG**
purA	GGCTTC**GAA**TACCA-N_{08}-TCAGC**TTC**ACCCT-N_{409}-**ATG**
ssb	GGTGGG**GAA**GGGAA-N_{09}-GACGG**TTC**AAAAG-N_{432}-**ATG**
atpA	GCCGAC**CAA**GGCCG-N_{09}-CGCGG**TTC**TGGAC-N_{353}-**ATG**
livK	GCTGCC**CAA**CACCG-N_{10}-CGGCC**TTC**GCAAG-N_{015}-**ATG**
COG2335	CCTGGC**GAA**ATCCT-N_{07}-GCGAT**TTC**CGCAC-N_{108}-**ATG**

Fig. 6. Identification of putative promoter motifs of RpoE2-dependent genes in *A. brasilense* Sp7. Upstream regions of the genes encoding upregulated proteins (listed in Table 2) were analysed using BioProspector. The sequence logo of the predicted promoter motif was generated using the WebLogo3 tool (http://weblogo.berkeley.edu/). Nucleotide sequences of the putative promoter −10 and −35 motifs (shown in bold type) are separated by a spacer of 17–19 bp.

R. sphaeroides. The conserved His141, His143, Glu147 and His177 residues that are involved in the binding of a Zn^{2+} ion in the CLD are required to promote dissociation of the σ^E–ChrR complex of *R. sphaeroides* and *C. crescentus* by $^1O_2$ and organic hydroperoxide (tert-butylhydroperoxide) (Greenwell *et al.*, 2011; Lourenço *et al.*, 2011). The two cysteine residues (Cys186 and Cys188) located at the extreme end of the CLD in the ChrR of *C. crescentus* and *R. sphaeroides* are also present in the two ChrR paralogues of *A. brasilense*. Although these cysteine residues of ChrR in *C. crescentus* have been shown to be critical for responding to cadmium stress (Lourenço *et al.*, 2011), they were not involved in promoting dissociation of the σ^E–ChrR complex of *R. sphaeroides* in response to cadmium stress (Greenwell *et al.*, 2011).

The deduced −10 and −35 elements of the Abr *rpoE2* promoter were identical neither to the constitutive (Abr *rpoE1*P1) nor to the inducible (Abr *rpoE1*P2) promoter motifs located upstream of the Abr *rpoE1* (Mishra *et al.*, 2011). The −35 motif (GAATCC) of the *rpoE2* promoter showed significant similarities to the consensus of the ECF11-type promoter (TGATCC-16-CGTA) as well as to the ECF12-type promoter (GGAAT-19-GTT) (Staroń *et al.*, 2009). The ECF11-type promoter consensus is found in Abr *rpoE1*P2, Rsp *rpoE* and in many other α-proteobacteria (Dufour *et al.*, 2008). The −10 sequence (CTA) of the *rpoE2* promoter was also similar to the GTA motif of the ECF11-type promoter consensus. The 2.3–2.4 and 4.2 regions of Abr RpoE2, which are known to recognize the −35 and −10 promoter motifs, respectively, showed a notable similarity to those of RpoE1 of *A. brasilense* and RpoE of *R. sphaeroides*. The observed lack of autoregulation and constitutive expression of *rpoE2* might be due to the deviation of the −35 motif of the *rpoE2* promoter from the consensus of an ECF11-type promoter. A similar lack of autoregulation was also observed earlier for the *rpoE* gene of *Xylella fastidiosa* (da Silva Neto *et al.*, 2007). Analysis of the upstream regions of the genes upregulated in the *chrR2*::Km mutant or in *A. brasilense* overexpressing *rpoE2* indicated a putative −35 and −10 promoter consensus, which showed similarity to the promoters dependent on ECF12, ECF15 or ECF27-type sigma factors (Staroń *et al.*, 2009). The predicted RpoE2-dependent promoter consensus, however, does not match the promoter consensus of RpoE1 of *A. brasilense* (Mishra *et al.*, 2011) and RpoE of *R. sphaeroides* (Dufour *et al.*, 2008). Thus, the absence of a putative RpoE2-dependent consensus in the upstream region of the *rpoE2–chrR2* operon is in agreement with the observed lack of its autoregulation.

To study the role of RpoE2 and ChrR2 in the physiology of *A. brasilense*, we constructed an *A. brasilense* strain overexpressing *rpoE2* and a *chrR2*::Km mutant, which allowed availability of free RpoE2 in the cell. One obvious phenotype of *chrR2*::Km as well as *A. brasilense* Sp7 overexpressing RpoE2 was the elevated levels of carotenoids compared with those produced by *A. brasilense* Sp7. The significantly higher level of carotenoid synthesis in *A. brasilense* Sp7 overexpressing *rpoE2* compared with that observed in the *chrR2*::Km mutant might be due to the enhanced level of RpoE2 in the former. The increased production of carotenoids in the *chrR2*::Km mutant and *A. brasilense* overexpressing *rpoE2* might reflect a mechanism to cope with photooxidative stress. This is reflected in the enhanced tolerance of the *chrR2*::Km mutant and *A. brasilense* Sp7 overexpressing RpoE2 to the two $^1O_2$-generating agents methylene blue and toluidine blue. Since toluidine blue is less specific for $^1O_2$ formation and exhibits a relatively lower quantum yield, the $^1O_2$ stress caused by toluidine blue is lower than that caused by methylene blue (Demidova & Hamblin, 2004; Wainwright & Giddens, 2003).

The *chrR2*::Km mutant and *A. brasilense* Sp7 overexpressing RpoE2 also showed remarkable resistance to the β-lactam antibiotics that cause cell envelope stress by inhibiting peptidoglycan biosynthesis, and to nalidixic acid, which inhibits DNA gyrase activity. Oxidative stress is also an end product of antimicrobial exposure. Therefore, the oxidative stress response is expected to promote resistance to antimicrobials (Poole, 2012). ECF sigma factors have been shown to confer resistance to antibiotics in Gram-positive bacteria (Cao *et al.*, 2002; Ho & Ellermeier, 2012; Luo *et al.*, 2010; Luo & Helmann, 2012; Mascher *et al.*, 2007; Ross *et al.*, 2009). Resistance to β-lactam antibiotics in *Streptococcus pneumoniae* has been shown to be due to stabilization of cell wall synthetic

enzymes by chaperones (Tran *et al.*, 2011). The *chrR2*::Km mutant and *A. brasilense* Sp7 overexpressing RpoE2 showed resistance to nalidixic acid, which is an inhibitor of gyrase activity. Depending upon the redox status of the cell, gyrase activity regulates gene expression by increasing supercoiling under reducing conditions and decreasing it under oxidizing conditions (Zeller & Klug, 2006; Zhu & Hearst, 1988).

In order to identify the genes and functions controlled by RpoE2–ChrR2, we identified proteins which were upregulated in *A. brasilense* Sp7 overexpressing RpoE2. The protein that was maximally upregulated (61-fold) in *A. brasilense* Sp7 overexpressing *rpoE2* was a fasciclin-domain protein. Although the role of fasciclin-domain proteins in bacteria is not clearly known, they are thought to be involved in cell envelope morphogenesis and cell adhesion, and are considered important in symbiosis (Paulsrud & Lindblad, 2002). Some of the upregulated proteins, such as GroEL, GroES, EF-Tu, EF-G and ClpP, are known to play important roles during heat stress, oxidative stress and photooxidative stress (Caldas *et al.*, 2000; Hartl & Hayer-Hartl, 2002; Vorderwülbecke *et al.*, 2004). Several of the upregulated proteins are also differentially expressed during photooxidative stress in *Roseobacter denitrificans* (Berghoff *et al.*, 2011) and *Sphingopyxis alaskensis* (Matallana-Surget *et al.*, 2009). While ATP synthase (AtpA) enables *A. brasilense* to cope with the ATP demands of protein synthesis, protein folding and DNA repair under stressful conditions (Proctor & von Humboldt, 1998; Zhang & Haldenwang, 2005), methionine transport proteins overcome methionine limitation due to oxidative inactivation of methionine synthase (MetE), the enzyme catalysing the final step in methionine biosynthesis (Hondorp & Matthews, 2004). Ketol-acid reductoisomerase (IlvC) is also induced by photooxidative stress in *Roseobacter denitrificans* and by cold shock in *Bacillus subtilis* (Berghoff *et al.*, 2011; Graumann *et al.*, 1996). Adenylosuccinate synthetase is known to replenish the total adenylate pool after oxidative damage of purines (Zhang & Haldenwang, 2005). Some of the upregulated proteins, for example GTP cyclohydrolase I, 50S ribosomal protein L9, chaperones GroES and GroEL, protease ClpP and single stranded DNA-binding proteins, have been shown to be involved in controlling the bacterial cell cycle (Grünenfelder *et al.*, 2001).

A. brasilense possesses a complex branched-chain electron transport system and oxidative type of metabolism involving the synthesis of haem-containing cytochromes (Alexandre *et al.*, 1999; Marchal *et al.*, 1998). During its movement from the rhizosphere to new environments, haem compounds of *A. brasilense* may be exposed to light and become a potential source of $^1O_2$, causing photooxidative stress and cell damage. RpoE2–ChrR2 seems to play a major role in minimizing the cell damage caused by photooxidative stress by enhancing the synthesis of carotenoids and chaperones in *A. brasilense*. Upregulation of adenylosuccinate synthetase by RpoE2 is an example of the role played by RpoE2 in repairing the damaged DNA. The involvement of RpoE2–ChrR2 in conferring resistance to some of the cell wall-acting antibiotics also suggests their important role in maintaining the shape and osmotic stability of the bacterial cell (Typas *et al.*, 2010). The lack of autoregulation and regulation by stress agents at the level of transcription of the *rpoE2–chrR2* operon suggests that the constitutively expressed RpoE2 and ChrR2 might regulate expression of their target genes by stress-mediated disruption of the RpoE2–ChrR2 complex (Greenwell *et al.*, 2011). The differences in the mechanisms of regulation of *rpoE1–chrR1* and *rpoE2–chrR2* suggest that the former may be responsible for long-term tolerance to stress whereas the latter might be important in a rapid response to stress. Our ongoing studies on the sensitivity of RpoE1–ChrR1 and RpoE2–ChrR2 protein complexes to different reactive oxygen species, and the possibilities of cross-talk between RpoE1–ChrR2 and RpoE2–ChrR1, are likely to provide more insights into the regulatory mechanisms that rhizobacteria might use in coping with oxidative stress.

ACKNOWLEDGEMENTS

This work was supported by a grant from the Department of Biotechnology, New Delhi to A. K. T. M. N. M. and N. G. were supported by fellowships from the Council of Scientific and Industrial Research, New Delhi and the University Grant Commission, New Delhi, respectively. We thank Igor Zhulin (University of Tennessee, Knoxville) for providing access to the *Azospirillum brasilense* Sp245 genome, and J. P. Gaur (Department of Botany, Banaras Hindu University) for reading the manuscript. Dedicated to the memory of Pt Madan Mohan Malviya, the founder of Banaras Hindu University, in the 150th anniversary of his birth.

REFERENCES

Alexandre, G., Bally, R., Taylor, B. L. & Zhulin, I. B. (1999). Loss of cytochrome *c* oxidase activity and acquisition of resistance to quinone analogs in a laccase-positive variant of *Azospirillum lipoferum*. *J Bacteriol* **181**, 6730–6738.

Alvarez-Martinez, C. E., Lourenço, R. F., Baldini, R. L., Laub, M. T. & Gomes, S. L. (2007). The ECF sigma factor σ^T is involved in osmotic and oxidative stress responses in *Caulobacter crescentus*. *Mol Microbiol* **66**, 1240–1255.

Anthony, J. R., Newman, J. D. & Donohue, T. J. (2004). Interactions between the *Rhodobacter sphaeroides* ECF sigma factor, σ^E, and its anti-sigma factor, ChrR. *J Mol Biol* **341**, 345–360.

Anthony, J. R., Warczak, K. L. & Donohue, T. J. (2005). A transcriptional response to singlet oxygen, a toxic byproduct of photosynthesis. *Proc Natl Acad Sci U S A* **102**, 6502–6507.

Baldani, J. I., Krieg, N. R., Baldani, V. L. D., Hartmann, A. & Dobereiner, J. (1979). Genus II. *Azospirillum* Tarrand, Krieg and Dobereiner, 79AL. In *Bergey's Manual of Systematic Bacteriology*, vol. 2. Edited by G. M. Garrity, D. J. Brenner, N. R. Krieg & J. T. Staley. New York: Springer.

Bang, I.-S., Frye, J. G., McClelland, M., Velayudhan, J. & Fang, F. C. (2005). Alternative sigma factor interactions in *Salmonella*: σ^E and σ^H promote antioxidant defences by enhancing σ^S levels. *Mol Microbiol* **56**, 811–823.

Berghoff, B. A., Glaeser, J., Nuss, A. M., Zobawa, M., Lottspeich, F. & Klug, G. (2011). Anoxygenic photosynthesis and photooxidative

stress: a particular challenge for *Roseobacter*. *Environ Microbiol* **13**, 775–791.

Brown, K. L. & Hughes, K. T. (1995). The role of anti-sigma factors in gene regulation. *Mol Microbiol* **16**, 397–404.

Caldas, T., Laalami, S. & Richarme, G. (2000). Chaperone properties of bacterial elongation factor EF-G and initiation factor IF2. *J Biol Chem* **275**, 855–860.

Cao, M., Wang, T., Ye, R. & Helmann, J. D. (2002). Antibiotics that inhibit cell wall biosynthesis induce expression of the *Bacillus subtilis* σ^{W} and σ^{M} regulons. *Mol Microbiol* **45**, 1267–1276.

Cogdell, R. J., Howard, T. D., Bittl, R., Schlodder, E., Geisenheimer, I. & Lubitz, W. (2000). How carotenoids protect bacterial photosynthesis. *Philos Trans R Soc Lond B Biol Sci* **355**, 1345–1349.

Crooks, G. E., Hon, G., Chandonia, J. M. & Brenner, S. E. (2004). WebLogo: a sequence logo generator. *Genome Res* **14**, 1188–1190.

da Silva Neto, J. F., Koide, T., Gomes, S. L. & Marques, M. V. (2007). The single extracytoplasmic-function sigma factor of *Xylella fastidiosa* is involved in the heat shock response and presents an unusual regulatory mechanism. *J Bacteriol* **189**, 551–560.

Demidova, T. N. & Hamblin, M. R. (2004). Photodynamic therapy targeted to pathogens. *Int J Immunopathol Pharmacol* **17**, 245–254.

Dufour, Y. S., Landick, R. & Donohue, T. J. (2008). Organization and evolution of the biological response to singlet oxygen stress. *J Mol Biol* **383**, 713–730.

Firoved, A. M., Boucher, J. C. & Deretic, V. (2002). Global genomic analysis of AlgU (σ^{E})-dependent promoters (sigmulon) in *Pseudomonas aeruginosa* and implications for inflammatory processes in cystic fibrosis. *J Bacteriol* **184**, 1057–1064.

Glaeser, J. & Klug, G. (2005). Photo-oxidative stress in *Rhodobacter sphaeroides*: protective role of carotenoids and expression of selected genes. *Microbiology* **151**, 1927–1938.

Glaeser, J., Nuss, A. M., Berghoff, B. A. & Klug, G. (2011). Singlet oxygen stress in microorganisms. *Adv Microb Physiol* **58**, 141–173.

Graumann, P., Schröder, K., Schmid, R. & Marahiel, M. A. (1996). Cold shock stress-induced proteins in *Bacillus subtilis*. *J Bacteriol* **178**, 4611–4619.

Greenwell, R., Nam, T. W. & Donohue, T. J. (2011). Features of *Rhodobacter sphaeroides* ChrR required for stimuli to promote the dissociation of σ^{E}/ChrR complexes. *J Mol Biol* **407**, 477–491.

Grünenfelder, B., Rummel, G., Vohradsky, J., Röder, D., Langen, H. & Jenal, U. (2001). Proteomic analysis of the bacterial cell cycle. *Proc Natl Acad Sci U S A* **98**, 4681–4686.

Haine, V., Dozot, M., Dornand, J., Letesson, J. J. & De Bolle, X. (2006). NnrA is required for full virulence and regulates several *Brucella melitensis* denitrification genes. *J Bacteriol* **188**, 1615–1619.

Hartl, F. U. & Hayer-Hartl, M. (2002). Molecular chaperones in the cytosol: from nascent chain to folded protein. *Science* **295**, 1852–1858.

Helmann, J. D. (2002). The extracytoplasmic function (ECF) sigma factors. *Adv Microb Physiol* **46**, 47–110.

Ho, T. D. & Ellermeier, C. D. (2012). Extra cytoplasmic function σ factor activation. *Curr Opin Microbiol* **15**, 182–188.

Hondorp, E. R. & Matthews, R. G. (2004). Oxidative stress inactivates cobalamin-independent methionine synthase (MetE) in *Escherichia coli*. *PLoS Biol* **2**, e336.

Kumar, K., Tharad, M., Ganapathy, S., Ram, G., Narayan, A., Khan, J. A., Pratap, R., Ghosh, A., Samuchiwal, S. K. & other authors (2009). Phenylalanine-rich peptides potently bind ESAT6, a virulence determinant of *Mycobacterium tuberculosis*, and concurrently affect the pathogen's growth. *PLoS ONE* **4**, e7615.

Liu, X., Brutlag, D. L. & Liu, J. S. (2001). BioProspector: discovering conserved DNA motifs in upstream regulatory regions of co-expressed genes. *Pac Symp Biocomput* **6**, 127–138.

Lourenço, R. F. & Gomes, S. L. (2009). The transcriptional response to cadmium, organic hydroperoxide, singlet oxygen and UV-A mediated by the σ^{E}-ChrR system in *Caulobacter crescentus*. *Mol Microbiol* **72**, 1159–1170.

Lourenço, R. F., Kohler, C. & Gomes, S. L. (2011). A two-component system, an anti-sigma factor and two paralogous ECF sigma factors are involved in the control of general stress response in *Caulobacter crescentus*. *Mol Microbiol* **80**, 1598–1612.

Luo, Y. & Helmann, J. D. (2012). Analysis of the role of *Bacillus subtilis* σ^{M} in β-lactam resistance reveals an essential role for c-di-AMP in peptidoglycan homeostasis. *Mol Microbiol* **83**, 623–639.

Luo, Y., Asai, K., Sadaie, Y. & Helmann, J. D. (2010). Transcriptomic and phenotypic characterization of a *Bacillus subtilis* strain without extracytoplasmic function σ factors. *J Bacteriol* **192**, 5736–5745.

Marchal, K., Sun, J., Keijers, V., Haaker, H. & Vanderleyden, J. (1998). A cytochrome cbb_3 (cytochrome *c*) terminal oxidase in *Azospirillum brasilense* Sp7 supports microaerobic growth. *J Bacteriol* **180**, 5689–5696.

Martínez-Salazar, J. M., Salazar, E., Encarnación, S., Ramírez-Romero, M. A. & Rivera, J. (2009). Role of the extracytoplasmic function sigma factor RpoE4 in oxidative and osmotic stress responses in *Rhizobium etli*. *J Bacteriol* **191**, 4122–4132.

Mascher, T., Hachmann, A. B. & Helmann, J. D. (2007). Regulatory overlap and functional redundancy among *Bacillus subtilis* extracytoplasmic function σ factors. *J Bacteriol* **189**, 6919–6927.

Matallana-Surget, S., Joux, F., Raftery, M. J. & Cavicchioli, R. (2009). The response of the marine bacterium *Sphingopyxis alaskensis* to solar radiation assessed by quantitative proteomics. *Environ Microbiol* **11**, 2660–2675.

Miller, J. H. (1972). *Experiments in Molecular Genetics*. Cold Spring Harbor, NY: Cold Spring Harbor Laboratory.

Mishra, M. N., Thirunavukkarasu, N., Sharma, I. M., Jagnnadham, M. V. & Tripathi, A. K. (2008). Mutation in a gene encoding anti-σ factor in *A. brasilense* confers tolerance to elevated temperature, antibacterial peptide and PEG-200 via carotenoid synthesis. *FEMS Microbiol Lett* **287**, 221–229.

Mishra, M. N., Kumar, S., Gupta, N., Kaur, S., Gupta, A. & Tripathi, A. K. (2011). An extracytoplasmic function sigma factor cotranscribed with its cognate anti-sigma factor confers tolerance to NaCl, ethanol and methylene blue in *Azospirillum brasilense* Sp7. *Microbiology* **157**, 988–999.

Morales, V. M., Bäckman, A. & Bagdasarian, M. (1991). A series of wide-host-range low-copy-number vectors that allow direct screening for recombinants. *Gene* **97**, 39–47.

Newman, J. D., Anthony, J. R. & Donohue, T. J. (2001). The importance of zinc-binding to the function of *Rhodobacter sphaeroides* ChrR as an anti-sigma factor. *J Mol Biol* **313**, 485–499.

Norman, R. A., Poh, C. L., Pearl, L. H., O'Hara, B. P. & Drew, R. E. (2000). Steric hindrance regulation of the *Pseudomonas aeruginosa* amidase operon. *J Biol Chem* **275**, 30660–30667.

Nur, I., Steinitz, Y. L., Okon, Y. & Henis, Y. (1981). Carotenoid composition and function in nitrogen-fixing bacteria of the genus *Azospirillum*. *J Gen Microbiol* **122**, 27–32.

Nuss, A. M., Glaeser, J., Berghoff, B. A. & Klug, G. (2010). Overlapping alternative sigma factor regulons in the response to singlet oxygen in *Rhodobacter sphaeroides*. *J Bacteriol* **192**, 2613–2623.

Paget, M. S. B., Bae, J.-B., Hahn, M.-Y., Li, W., Kleanthous, C., Roe, J.-H. & Buttner, M. J. (2001). Mutational analysis of RsrA, a

zinc-binding anti-sigma factor with a thiol-disulphide redox switch. *Mol Microbiol* **39**, 1036–1047.

Park, S.-D., Youn, J.-W., Kim, Y.-J., Lee, S.-M., Kim, Y. & Lee, H.-S. (2008). *Corynebacterium glutamicum* σ^{E} is involved in responses to cell surface stresses and its activity is controlled by the anti-σ factor CseE. *Microbiology* **154**, 915–923.

Paulsrud, P. & Lindblad, P. (2002). Fasciclin domain proteins are present in nostoc symbionts of lichens. *Appl Environ Microbiol* **68**, 2036–2039.

Poole, K. (2012). Stress responses as determinants of antimicrobial resistance in Gram-negative bacteria. *Trends Microbiol* **20**, 227–234.

Proctor, R. A. & von Humboldt, A. (1998). Bacterial energetics and antimicrobial resistance. *Drug Resist Updat* **1**, 227–235.

Ravanat, J. L., Martinez, G. R., Medeiros, M. H., Di Mascio, P. & Cadet, J. (2004). Mechanistic aspects of the oxidation of DNA constituents mediated by singlet molecular oxygen. *Arch Biochem Biophys* **423**, 23–30.

Ross, C. L., Thomason, K. S. & Koehler, T. M. (2009). An extracytoplasmic function sigma factor controls β-lactamase gene expression in *Bacillus anthracis* and other *Bacillus cereus* group species. *J Bacteriol* **191**, 6683–6693.

Rowen, D. W. & Deretic, V. (2000). Membrane-to-cytosol redistribution of ECF sigma factor AlgU and conversion to mucoidy in *Pseudomonas aeruginosa* isolates from cystic fibrosis patients. *Mol Microbiol* **36**, 314–327.

Rowley, G., Spector, M., Kormanec, J. & Roberts, M. (2006). Pushing the envelope: extracytoplasmic stress responses in bacterial pathogens. *Nat Rev Microbiol* **4**, 383–394.

Schurr, M. J., Yu, H., Martinez-Salazar, J. M., Boucher, J. C. & Deretic, V. (1996). Control of AlgU, a member of the σ^{E}-like family of stress sigma factors, by the negative regulators MucA and MucB and *Pseudomonas aeruginosa* conversion to mucoidy in cystic fibrosis. *J Bacteriol* **178**, 4997–5004.

Simon, R., Priefer, U. & Pühler, A. (1983). A broad host range mobilization system for *in vivo* genetic engineering: transposon mutagenesis in Gram negative bacteria. *Biotechnology* **1**, 784–791.

Staroń, A., Sofia, H. J., Dietrich, S., Ulrich, L. E., Liesegang, H. & Mascher, T. (2009). The third pillar of bacterial signal transduction: classification of the extracytoplasmic function (ECF) σ factor protein family. *Mol Microbiol* **74**, 557–581.

Steenhoudt, O. & Vanderleyden, J. (2000). *Azospirillum*, a free-living nitrogen-fixing bacterium closely associated with grasses: genetic, biochemical and ecological aspects. *FEMS Microbiol Rev* **24**, 487–506.

Thakur, K. G., Jaiswal, R. K., Shukla, J. K., Praveena, T. & Gopal, B. (2010). Over-expression and purification strategies for recombinant multi-protein oligomers: a case study of *Mycobacterium tuberculosis* σ/anti-σ factor protein complexes. *Protein Expr Purif* **74**, 223–230.

Thirunavukkarasu, N., Mishra, M. N., Spaepen, S., Vanderleyden, J., Gross, C. A. & Tripathi, A. K. (2008). An extra-cytoplasmic function sigma factor and anti-sigma factor control carotenoid biosynthesis in *Azospirillum brasilense*. *Microbiology* **154**, 2096–2105.

Tran, T. D., Kwon, H. Y., Kim, E. H., Kim, K. W., Briles, D. E., Pyo, S. & Rhee, D. K. (2011). Decrease in penicillin susceptibility due to heat shock protein ClpL in *Streptococcus pneumoniae*. *Antimicrob Agents Chemother* **55**, 2714–2728.

Typas, A., Banzhaf, M., van den Berg van Saparoea, B., Verheul, J., Biboy, J., Nichols, R. J., Zietek, M., Beilharz, K., Kannenberg, K. & other authors (2010). Regulation of peptidoglycan synthesis by outer-membrane proteins. *Cell* **143**, 1097–1109.

Vanstockem, M., Michiels, K., Vanderleyden, J. & Van Gool, A. P. (1987). Transposon mutagenesis of *Azospirillum brasilense* and *Azospirillum lipoferum*: physical analysis of Tn*5* and Tn*5*-mob insertion mutants. *Appl Environ Microbiol* **53**, 410–415.

Vorderwülbecke, S., Kramer, G., Merz, F., Kurz, T. A., Rauch, T., Zachmann-Brand, B., Bukau, B. & Deuerling, E. (2004). Low temperature or GroEL/ES overproduction permits growth of *Escherichia coli* cells lacking trigger factor and DnaK. *FEBS Lett* **559**, 181–187.

Wainwright, M. & Giddens, R. M. (2003). Phenothiazinium photosensitisers: choices in synthesis and application. *Dyes Pigments* **57**, 245–257.

Wisniewski-Dyé, F., Borziak, K., Khalsa-Moyers, G., Alexandre, G., Sukharnikov, L. O., Wuichet, K., Hurst, G. B., McDonald, W. H., Robertson, J. S. & other authors (2011). *Azospirillum* genomes reveal transition of bacteria from aquatic to terrestrial environments. *PLoS Genet* **7**, e1002430.

Yoshimura, M., Asai, K., Sadaie, Y. & Yoshikawa, H. (2004). Interaction of *Bacillus subtilis* extracytoplasmic function (ECF) sigma factors with the N-terminal regions of their potential anti-sigma factors. *Microbiology* **150**, 591–599.

Zeller, T. & Klug, G. (2006). Thioredoxins in bacteria: functions in oxidative stress response and regulation of thioredoxin genes. *Naturwissenschaften* **93**, 259–266.

Zhang, S. & Haldenwang, W. G. (2005). Contributions of ATP, GTP, and redox state to nutritional stress activation of the *Bacillus subtilis* σ^{B} transcription factor. *J Bacteriol* **187**, 7554–7560.

Zhu, Y. S. & Hearst, J. E. (1988). Transcription of oxygen-regulated photosynthetic genes requires DNA gyrase in *Rhodobacter capsulatus*. *Proc Natl Acad Sci U S A* **85**, 4209–4213.

Ziegelhoffer, E. C. & Donohue, T. J. (2009). Bacterial responses to photo-oxidative stress. *Nat Rev Microbiol* **7**, 856–863.

Edited by: M. F. Hynes